# LEO-Assisted Beidou B1C Signal Acquisition Algorithm and On-Orbit Verification

Wei Zhang[1,2(✉)], Qijia Dong[2], Shuangna Zhang[2], Li Tian[1,2], Kun Liu[1,2], and Jinshan Liu[1,2]

[1] Tianjin Zhong Wei Aerospace Data System Technology Co., Ltd., Tianjin 300301, China
[2] Space Star Technology Co., Ltd., Beijing 100086, China

**Abstract.** In the occlusion and electromagnetic interference environment, the GNSS navigation signal is seriously attenuated, and traditional GNSS receivers are difficult to capture. For direct capture of weak signals, long-time coherent integration and non-coherent integration can be used to improve the signal-to-noise ratio (SNR) of the signal. However, coherent integration time is limited and bit flipping, and non-coherent integration has a square loss, resulting in a significant increase in the SNR. Taking into account the advantages of LEO satellites with low orbital height and large landing power, this paper proposes a LEO-assisted acquisition algorithm. The code phase and Doppler frequency estimates can be obtained through the assistance of LEO satellites, which can extend the coherent integration time. This method can effectively improve the anti-interference ability of the B1C signal and reduce the average acquisition time. The on-orbit test results show that under the condition of 80 ms coherent integration and 2 times incoherent, B1C anti-interference ability can be improved by 14 dB.

**Keywords:** LEO-assisted · Acquisition · Anti-interference · On-orbit

## 1 Introduction

On July 31, 2020, the BDS-3 global satellite navigation system was officially opened for use, which can provide users around the world with all-day, continuous and uninterrupted navigation and positioning services, and is widely used in military and civilian fields. Although BDS-3 has been built, due to the inherent shortcomings of the satellite navigation system, BDS, like GPS and other global navigation satellite systems (GNSS), naturally has shortcomings. Moreover, with the gradual expansion of satellite navigation applications and the continuous improvement of users' demand for service accuracy, especially in the fields of autonomous driving, homeland survey, military and national defense, the vulnerability of GNSS navigation signals has become more prominent [1, 2]. GNSS satellite orbit height is above 20000 km. On the one hand, due to the limitation of the energy on the satellite, it cannot transmit high-power signals; on the other hand, the navigation signal undergoes radio frequency attenuation and electromagnetic interference during long-distance propagation, and the signal is already very


X. Wang et al. (Eds.): AICON 2021, LNICST 396, pp. 153–164, 2021.
https://doi.org/10.1007/978-3-030-90196-7_14

weak when it reaches the ground, only about −160 dbW [3]. Moreover, in practical applications, GNSS navigation signals are widely used in weak signal environments, including urban indoors, forests, mountains, canyons, tunnels, underground garages, etc. The carrier to noise ratio (CN0) of satellite signals in these environments is about 15 dB lower than that in an open outdoor environment. The acquisition sensitivity of traditional receivers is difficult to meet the acquisition requirements of weak signals in these complex environments.

For weak signal capture technology, coherent integration and non-coherent integration are the classic weak signal capture methods [4]· The coherent integration method can obtain the maximum signal-to-noise ratio gain. However, the coherent integration is limited by the influence of the navigation data bit flip, and the coherent integration time usually cannot exceed the length of one navigation data bit. Although the non-coherent integration method can overcome the impact of bit jumps, its disadvantage is that there is a square loss. In view of the shortcomings of the above-mentioned direct acquisition method, this paper proposes a LEO satellite to assist BDS B1C weak signal acquisition algorithm, through the LEO satellite to obtain code phase estimates and doppler estimates to extend the coherent integration time, improve the weak signal capture ability.

## 2 System Model

With the continuous development of navigation application requirements such as artificial intelligence, Internet of Things, and autonomous driving, LEO satellites have become a hot issue in the construction of satellite navigation systems in recent years due to their excellent signal characteristics and application potential. LEO satellites can enhance satellite navigation signals as an enhancement and supplement to GNSS. They can also broadcast independent ranging signals through the integration of communication systems and navigation systems to form backup positioning and navigation capabilities. Iridium in the United States has realized the integration and development of GPS systems, providing users with STL (Satellites Time and Location) services, which can back up and enhance GPS capabilities [5]. China has also built and deployed its own low-orbit navigation constellation, the "ongYan" constellation constructed by China Aerospace Science and Technology Corporation, the "HongYun" project planned by China Aerospace Science and Industry Corporation, and the "LuoJia-1" scientific experiment satellite developed by Wuhan University [6] and many more.

Compared with the current networked medium and high orbit satellite navigation system, the application of LEO satellite signals in navigation and positioning has the following advantages: First, the orbital height of LEO satellites is lower, which is about 5% of that of conventional GNSS satellites. One part, the free propagation loss of the signal is small, so the signal received on the ground is stronger; second, the LEO satellites are faster, the Doppler change is fast, and the geometric pattern changes quickly, which is conducive to the use of Doppler for positioning [7, 8]. Third, the research and development cost of LEO satellites and rocket launch costs are relatively low, and they can be launched by multiple satellites with one rocket (Fig. 1).

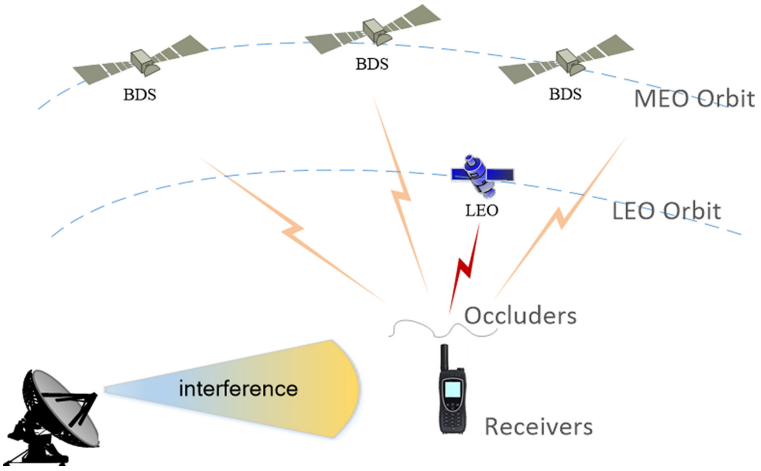


**Fig. 1.** Schematic diagram of the LEO navigation enhancement system

The LEO navigation enhancement system designed in this paper includes GNSS constellations, LEO satellites and ground navigation enhancement terminals.

The GNSS constellation transmits GNSS navigation signals. LEO satellites carry navigation enhancement payloads, forward the ephemeris of BDS satellites, and broadcast navigation enhancement signals. First, the LEO satellite receives and processes the GNSS navigation signal, and completes its own positioning based on the GNSS satellite signal, and at the same time obtains the ephemeris information of the BDS satellite. Then the ephemeris information of the BDS satellite is modulated into the LEO navigation enhancement signal and broadcasted to the ground navigation enhancement terminal.

The ground navigation enhancement terminal firstly performs independent positioning and timing by receiving the navigation enhancement signal of the LEO satellite. Then obtain the ephemeris of the forwarded BDS satellite through decoding. Finally, the auxiliary information is obtained by calculation, including the Doppler estimation value and code phase estimation value of the B1C signal, which assists in the realization of the B1C weak signal acquisition and completes more accurate positioning and timing services.

## 3 Algorithm Model

### 3.1 B1C Signal Model

**Signal Structure.** Compared with the BPSK single-channel signal system of BDS-2, the BDS-3 B1C signal adopts a new BOC modulation method, and at the same time, it has also been improved from a traditional single data channel to a data and pilot dual-channel structure. The data channel modulates a navigation message containing ranging information, while the pilot channel does not contain any data information. The baseband signal expression is as follows [3]:

$$S_{B1c\_Data}(t) = A_1 D(t) C_{Data}(t) sc_{Data}(t) \tag{1}$$

$$S_{B1c\_Pilot}(t) = A_2 C_{Pilot}(t) sc_{Pilot}(t) \tag{2}$$

Where, $A_1$ and $A_2$ are the amplitude of the data component and the pilot component respectively; $D(t)$ is the navigation message data of the B1C signal; $C_{Data}(t)$ and $C_{Pilot}(t)$ are the ranging code sequences of the data component and the pilot component respectively; $sc_{Data}(t)$ is the subcarrier of the data component; $sc_{Pilot}(t)$ is the subcarrier of the pilot component.

**Ranging Code Structure.** The B1C ranging codes are the tiered codes which are generated by XORing the primary codes with secondary codes. The B1C primary codes (for both data and pilot components) have the same chip rate of 1.023 Mcps, and have the same length of 10230 chips. The secondary code for each B1C pilot component has the length of 1800 chips. As shown in Fig. 2, The chip width of the secondary code has the same length as one period of a primary code, and the start of a secondary code chip is strictly aligned with the start of the first chip of primary code (Fig. 2).

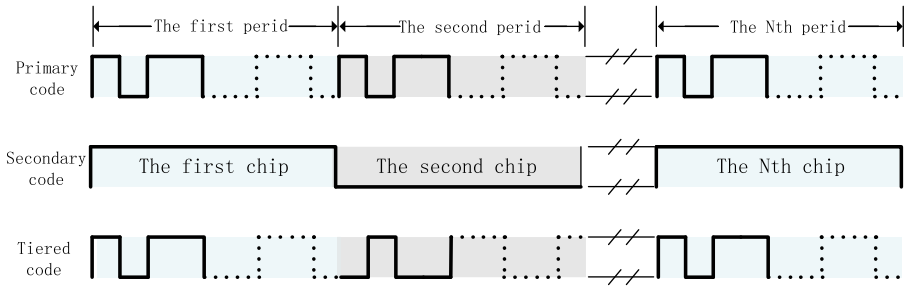


**Fig. 2.** Timing relationships of the primary code and secondary code

### 3.2 Algorithm Design

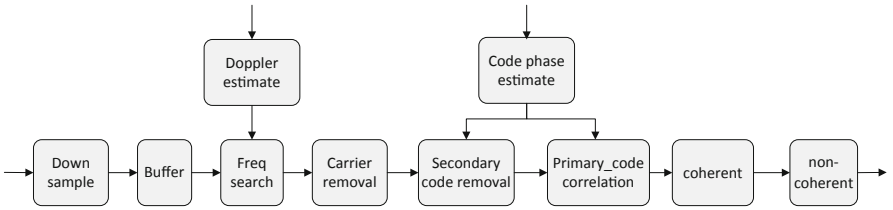


**Fig. 3.** Schematic diagram of the B1C acquisition algorithm assisted by LEO

Since the landing power of LEO satellites is generally 10-30dB higher than that of BDS satellites, ground terminals can still receive LEO navigation enhancement signals normally under B1C signal obstruction or interference. Considering the advantages and disadvantages of coherent integration and non-coherent integration, this paper designs

a LEO-assisted B1C acquisition algorithm for weak B1C signals, which is shown in Fig. 3. The algorithm uses the assistance of LEO satellites to achieve the acquisition of weak B1C signals by extending the coherent integration time as the main method and non-coherent as the auxiliary method.

According to Sect. 3.1, the data component of the B1C signal and the signal of the pilot component are synchronized. Moreover, the pilot component does not modulate the navigation message, so only capturing the pilot component can complete the capture of the B1C signal. Although the pilot component does not modulate the navigation message, it modulates the secondary code. This article uses LEO's auxiliary information to strip the secondary code of the pilot component to achieve long-term coherent integration.

**Get auxiliary information.** First, the ground navigation enhancement terminal uses the LEO navigation enhancement signal to independently complete coarse positioning and coarse timing, and at the same time obtain the retransmitted ephemeris of the visible BDS satellite. Taking into account the low orbital height of LEO and the large Doppler frequency deviation (usually around ±40 kHz), the LEO signal is captured using a parallel code algorithm, the frequency search step is set to 400 Hz, and the total integration accumulation time is 2 ms, so that the capture time can be Within 1 s.

Then, according to the results of coarse positioning and coarse timing and the transmitted ephemeris of the visible BDS satellite, comprehensively considering the receiver clock offset, clock drift and other factors, the Doppler and code phase estimates of the BDS B1C visible satellite are calculated.

**Acquisition of weak B1C signals by auxiliary information.** As shown in Fig. 3, the LEO-assisted B1C capture algorithm includes Down sample, Buffer, Freq search, Carrier removal, Secondary code removal, Primary_code correlation, coherent, non-coherent and so on. The ground navigation enhancement terminal uses the Doppler estimate to reduce the frequency search range when searching for frequencies. Using the code phase estimation value, on the one hand, the secondary code is stripped before the correlation operation, eliminating the limitation of "bit flip", and long-time coherent integration; on the other hand, the code phase search range is reduced during the main code correlation operation, saving hardware resources.

In order to improve the efficiency of acquisition, a parallel code acquisition method based on DBZP (Double Block Zero Padding) and FFT is used in the FPGA acquisition design. After the signal is mixed and down-converted to baseband, the received sequence is double-filled by the double-block zero-filling method, and then correlated with the local sequence. The correlation operation is realized by the FFT/IFFT module of the classic acquisition method of PCS (parallel code search), and then the correlation operation results are stored in RAM. For long-time coherent integration, the segment correlation accumulation operation is adopted to accumulate and store the correlation results of the same code phase. Then the stored coherent accumulation results are sequentially read out, and the IFFT operation is performed. Finally, the result is modulated and accumulated to complete the incoherent integration, and the peak value is compared with the threshold to complete the acquisition.

In addition, although the aiding information from LEO can narrow the search range of frequency and code phase, the longer the coherent integration time, the smaller the frequency search step. Under the same Doppler frequency offset, the number of frequency grids to be searched increases, which will increase the acquisition time to a certain extent. Moreover, after long-time coherent integration is used, the data sampling time is the main part of the acquisition time. In order to reduce the acquisition time and improve the

acquisition efficiency, this paper designs the use of a large-capacity buffer to store the amount of data required to complete a acquisition in advance, reducing the subsequent sampling time.

### 3.3 Determination of Integration Time

In order to enhance the filtering effect, reduce noise and improve sensitivity, the longer the coherent integration time, the better for improving the capture sensitivity. However, the determination of the coherent integration time requires comprehensive consideration from the following aspects:

(1) As the coherent integration time is lengthened, the crystal noise of the receiver will accumulate as a frequency deviation, which will cause the attenuation of the integral gain;
(2) The longer the coherent integration time, the greater the frequency error caused by the frequency stability of the receiver clock and the satellite clock, and the greater the coherent integration loss;
(3) The longer the coherent integration time, the smaller the frequency search step and the greater the amount of calculation;
(4) In order to maintain the dynamic response performance of the receiver, including the dynamics of satellite motion and clock noise, the integration result of the coherent integration needs to leave a certain bandwidth, and the coherent integration time cannot be too large.

After Matlab simulation analysis, with the assistance of LEO satellites, this article uses 80 ms coherent integration time and 2 non-coherent integrations to capture, which can take into account the noise and dynamic performance of the receiver, while balancing the coherent integration gain and the amount of calculation.

## 4 On-Orbit Verification

### 4.1 Testing Platform

In order to verify the effectiveness of the LEO-assisted B1C acquisition algorithm for improving the anti-jamming performance, this paper carried out an on-orbit test for experimental verification and analysis. The equipment required for the ground test verification platform mainly includes GNSS and LEO receiving antennas, anti-jamming navigation receivers, interference generators, combiners, computers, etc. GNSS and LEO receiving antennas are used to receive GNSS navigation signals and LEO navigation enhancement signals. The anti-jamming navigation receiver receives and processes the GNSS/LEO signal to complete the acquisition, tracking, positioning and calculation. The interference generator generates interference signals and sends them to the combiner for anti-interference testing. The combiner combines the signal received by the antenna with the interference signal to transmit the anti-jamming navigation receiver. The computer displays the test results and stores the test data.

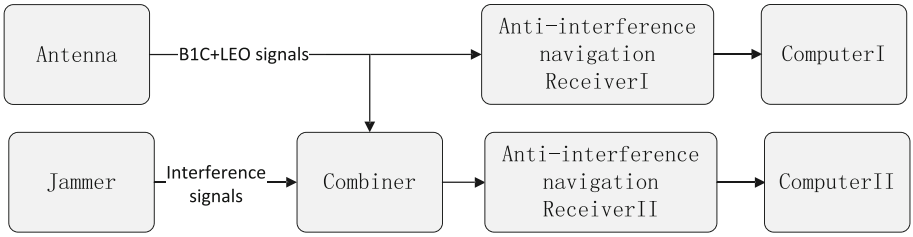


**Fig. 4.** On-orbit test equipment connection diagram

In order to verify the anti-jamming characteristics, this paper designed a ground test platform for on-orbit tests, as shown in Fig. 4. Receiver I is a non-interference on-orbit test, only receiving navigation signals, using the normal acquisition mode without assistance, as a reference and result comparison. Receiver II is an anti-jamming in-orbit test. Before LEO enters the test site, Receiver II uses the normal acquisition mode without assistance. The purpose is to test the anti-jamming performance of the acquisition algorithm without external assistance. When the LEO enters the visual range of the test site, the acquisition mode of the Receiver II is switched to the anti-jamming acquisition mode, in order to test the anti-jamming performance of the acquisition algorithm assisted by the LEO.

### 4.2 Testing Process

For the test platform shown in Fig. 4, the corresponding test process is designed in this section. Assume that T0 is the entry time of the LEO in orbit. For Receiver I, it only needs to be turned on 15 min before the entry of LEO, and use the normal mode to capture B1C. The test results of the Receiver I, including the captured satellite's PRN, CN0, Doppler, etc. And they will be used as the benchmark standard for the Receiver II. In order to verify the performance of LEO-assisted B1C acquisition, the test procedure of Receiver II is specifically designed as follows:

(1) T0–15 min time: Turn on Receiver II and keep the jammer off. The B1C signal works in the normal acquisition mode, and it is expected that multiple visible satellites will be successfully acquired.
(2) T0–12 min: Turn on the jammer and set a high-power jamming signal to ensure that the B1C signal is out of lock and cannot be positioned.
(3) T0–10 min: Adjust the jammer, reduce the signal power of the jamming signal by dB, and test the anti-jamming performance of the B1C normal capture mode. When B1C successfully captures using the normal capture mode, it records the signal power of the current interference signal. According to the calibration of the signal power in the budget, the anti-interference threshold of the normal mode is calculated.
(4) T0–5 min time: adjust the jammer and set high-power jamming signal to ensure that the B1C signal is out of lock and cannot be positioned.

(5) T0 time: LEO is visible, it is expected that the LEO signal acquisition will be successful, and the Doppler positioning will be completed within 1 min, and the B1C acquisition will be guided.
(6) T0 + 1 min time: adjust the jammer, reduce the signal power of the jamming signal by dB, and test the anti-jamming performance in the B1C anti-jamming capture mode. When B1C uses the anti-interference acquisition mode to successfully capture, record the signal power of the current interference signal power. According to the calibration of the signal power in the budget, the anti-jamming threshold of the anti-jamming mode is calculated.

Since the LEO satellite can be seen for about 10 min, the time is very short. During the on-orbit test, the test process of steps (3) and (6) is relatively time-consuming. Therefore, before the on-orbit test, the anti-interference ability of the terminal using GNSS and LEO signal simulation sources was used to conduct a threshold test. It only needs to test near the threshold.

The test process using GNSS/LEO signal simulator is the same as above. Without the aid of LEO satellites, test the acquisition situation of the anti-jamming receiver under different interference power conditions in the normal acquisition mode. After testing, the terminal capture interference signal ratio (ISR) threshold is 28 dBc. Under LEO-assisted conditions, test the anti-jamming terminal's anti-jamming mode under different interference power conditions. After testing, the terminal positioning ISR threshold is 42 dBc, compared with no LEO satellite guidance, anti-jamming The ability is increased by 14 dB.

### 4.3 On-Orbit Test and Results

On December 9, 2020, in Beijing, China, a ground receiving test was conducted on a LEO satellite signal in orbit. The visible time range of the LEO test satellite is 21:03:07–21:12:07, and the duration is 540 s.

**LEO Signal Power Test.** Normally and continuously LEO signals were received within the visible time. After successful acquisition and stable tracking, as shown in the Fig. 5, the satellite's elevation angle to the ground varies from 9° to 35°, and the statistical CN0 is from 47 dB-Hz to 63 dB-Hz. According to the positive correlation between the channel CN0 and the elevation angle, the CN0 will be even greater when the LEO satellite passes from the top, about 70 dB-Hz. In the Fig. 5, the start time of the time count on the horizontal axis is 21:03:59, which corresponds to 52 s after the entry of the LEO satellite. The elevation angle of the BDS satellite to the ground varies between 5° and 90°, and the CN0 is generally between 37 dB-Hz and 50 dB-Hz. It can be verified that the CN0 of LEO is about 10–20 dB higher than that of GNSS satellites, which is feasible for assisting B1C weak signal acquisition.

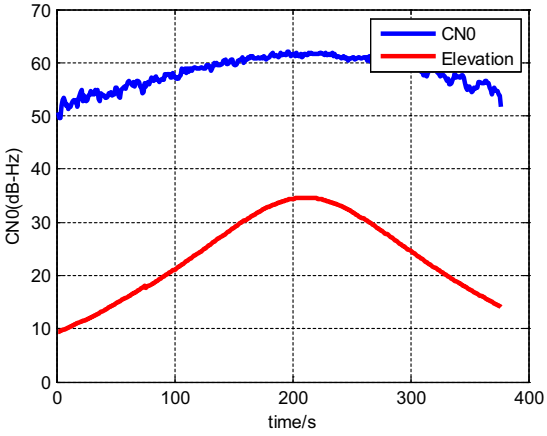


**Fig. 5.** CN0 and elevation angle of the LEO navigation signal

**Anti-interference Ability Test.** The anti-jamming capability test will begin 15 min before the LEO test satellite becomes visible. The test process and recorded results are shown in Table 1. In a non-interference scenario, anti-jamming Receiver I and Receiver II normally receive signals from 8 BDS satellites. The satellites are PRN23, PRN 24, PRN 25, PRN 34, PRN 39, PRN 40, PRN 43, and PRN 44.

The meanings of some abbreviations in Table 1 are as follows:
ACQ_OK: successful acquisition.
TRK_POS_OK: stable tracking and complete positioning.
LOSE_LOCK: the signal is in lock-out and recapture state.
AACQ: LEO is assisting B1C acquisition.

At 20:51:07, the interference value configuration of Receiver II is performed by the method described in Sect. 4.2, and ISR is set to 50 dbc. After the interference is turned on, the successfully captured satellites all lose lock, and the terminal enters the non-positioning state. When the interference signal power is adjusted and ISR is set to 28 dbc, the B1C acquisition in normal mode successfully captures multiple BDS satellites, indicating that the anti-jamming capability of the B1C acquisition without assistance in the orbit test is 28 dbc.

At 20:58:07, the anti-jamming test assisted by LEO is ready to be carried out, the ISR is set to 50dbc, and the successfully captured satellites lose lock again, and the Receiver II is in a non-positioning state. At 21:03:07, LEO can be seen, and the anti-jamming Receiver II starts to capture, track and Doppler single-satellite positioning of LEO. At 21:06:35, the positioning accuracy reached the level of guiding B1C, and the B1C acquisition began to be guided. At 21:07:42, when the ISR is set to 42 dbc, the B1C acquisition in anti-jamming mode successfully captured 6 satellites, indicating that the anti-jamming capability of B1C capture with the assistance of LEO in the orbit test is 42 dbc.

Table 2 shows the statistics of CN0 and elevation angle of BDS satellites captured by Receiver I without interference and Receiver II with interference.

**Table 1.** Test process and record results of Receiver II.

| Time | Jammer | | LEO | BDS B1C |
|---|---|---|---|---|
| | State | ISR (dbc) | | |
| 20:48:07 | OFF | --- | Invisible | Power on |
| 20:48:53 | OFF | --- | Invisible | ACQ_OK |
| 20:49:45 | OFF | --- | Invisible | TRK_POS_OK |
| 20:51:07 | ON | 50 | Invisible | LOSE_LOCK |
| 20:51:15 | Power down | 29 | Invisible | LOSE_LOCK |
| 20:53:07 | Power down | **28** | Invisible | ACQ-OK |
| 20:58:07 | Power up | 50 | Invisible | LOSE_LOCK |
| 21:03:07 | Power hold | 50 | Visible | LOSE_LOCK |
| 21:03:15 | Power hold | 50 | ACQ_OK | LOSE_LOCK |
| 21:03:59 | Power hold | 50 | TRK_POS_OK | LOSE_LOCK |
| 21:06:35 | Power hold | 50 | AACQ | LOSE_LOCK |
| 21:06:50 | Power down | 43 | AACQ | LOSE_LOCK |
| 21:07:42 | Power down | **42** | AACQ | ACQ_OK |
| 21:08:27 | Power hold | 42 | AACQ | TRK_POS_OK |
| 21:12:07 | Power hold | 42 dbc | Invisible | TRK_POS_OK |

**Table 2.** Comparison of B1C acquisition results with or without interference scenes

| PRN | Receiver I | | Receiver II | | |
|---|---|---|---|---|---|
| | CN0 (dB-Hz) | Elevation (°) | CN0 (dB-Hz) | Elevation (°) | ISR (dbc) |
| 23 | 48.3 | 53.34 | 36.6 | 60.72 | 28.5 |
| 24 | 36.1 | 14.74 | 25.8 | 8.69 | 39 |
| 25 | 48.6 | 70.83 | 35.8 | 63.66 | 29 |
| 28 | --- | --- | 27.0 | 18.31 | 38 |
| 34 | 48.4 | 58.59 | --- | --- | --- |
| 37 | --- | --- | 23.0 | 9.77 | 42 |
| 39 | 38.2 | 22.29 | 24.8 | 18.07 | 40 |
| 40 | 46.8 | 64.86 | --- | --- | --- |
| 43 | 48.2 | 61.99 | --- | --- | --- |
| 44 | 35.9 | 7.51 | --- | --- | --- |

In a non-interference scenario, Receiver I captures 8 satellites, of which PRN28 and PRN37 are not captured. According to the results captured by Receiver II, the elevation angles of the two satellites to the ground are small, and the signal CN0 is also small, which is limited by the acquisition sensitivity and probability of capture, so Receiver I failed to capture them.

In the interference scenario, the anti-interference acquisition mode captures 6 satellites, the elevation angle of PRN37 is 9.77°, the CN0 is 23.0 dB-Hz, the ISR is 42 dBc. And the CN0 of the remaining 5 satellites is higher than 23 dB.It should be noted that the PRN34, PRN40, PRN43, and PRN44 satellites were successfully captured in the non-interference scenario, but the anti-interference acquisition mode capture in the interference scenario failed to capture. After analyzing the forwarding strategy of satellite selection on the satellite, affected by factors including the validity of the ephemeris and the upper limit of the forwarding ephemeris, the above-mentioned satellites could not be forwarded to the ground by LEO, so the anti-jamming mode could not be captured.

In summary, the BDS satellites forwarded by LEO are visible to the ground. The ground anti-jamming receiver can complete the acquisition of the weak B1C signal according to the LEO forwarding BDS satellite ephemeris. In the non-interference scenario, the anti-interference ability of the normal acquisition mode is 28 dbc, and in the interference scene, the anti-interference ability of t anti-interference acquisition mode is 42 dbc. It shows that the anti-jamming performance of the LEO-assisted B1C acquisition algorithm proposed in this paper is very effective. The on-orbit test shows that the anti-jamming ability of the LEO-assisted B1C acquisition algorithm is improved by 14 dB.

## 5 Conclusion

This article analyzes the vulnerability of GNSS under occlusion and interference environments, and compares the effects of coherent integration and incoherent integration on the signal processing gain. Considering the development and advantages of LEO satellites, it is concluded that the acquisition algorithm that increases the coherent integration time with the aid of the low-orbit navigation enhancement signal is more effective for the acquisition of B1C signals under the condition of low SNR. Based on this, this paper designs a low-orbit navigation enhancement system, and proposes a LEO-assisted B1C acquisition algorithm, and analyzes the effectiveness and feasibility of the LEO-assisted acquisition algorithm from various aspects such as system design and algorithm principles. Finally, through the on-orbit test analysis of an on-orbit test satellite, it is obtained that the anti-jamming capability of the B1C signal with the assistance of LEO can be increased by 14 dB, which is of great significance for improving the anti-jamming performance of the GNSS signal.

## References

1. Zhao, Yu.: Brief probe on application of compass navigation satellite system in the fields of sea, land and air. In: Proceedings of 2017 2nd International Conference on Materials Science, Machinery and Energy Engineering, pp. 212–217.Dalian, China (2017)

2. Yang, Y.: Concepts of comprehensive PNT and related key technologies. Acta Geodaetica et Cartographica Sinica **45**(5), 505–510 (2016)
3. BeiDou Navigation Satellite System Signal in Space Interface Control Document Open Service Signal B1C (Version 1.0). http://www.beidou.gov.cn. Accessed 21 Apr 2021
4. Yang, C., Miller, M., Blasch, E., Blasch, E.: Comparative study of coherent non-coherent and semi-coherent integration schemes for GNSS receivers. Proc. ION GNSS **1**(2), 572 (2007)
5. Satelles-White-Paper-Final. https://satelles.com/wp-content/uploads/pdf/Satelles-White-Paper-2019.pdf. Accessed 21 Apr 2021
6. Tian, R., Cui, Z.-y., Zhang, S., Wang, D.: Navigation positioning & timing **1**(8), 66–81 (2021)
7. Zhizhong, L., Yu, Z., Xueli, Z., Yan, C.: Research and simulation of single star positioning algorithm based on low earth orbit satellite. In: Proceeding of 9th China Satlellite Navigation Conference. Ha'er bin China (2018)
8. Qin, H., Tan, Z., Cong, L., Zhao, C.: Positioning technology based on IRIDIUM signals of opportunity. J. Beijing Univ. Aeronaut. Astronaut. **45**(09), 1691–1699 (2019)